Article

Developmental Cell

Mitotic Membrane Turnover Coordinates Differential Induction of the Heart Progenitor Lineage

Graphical Abstract

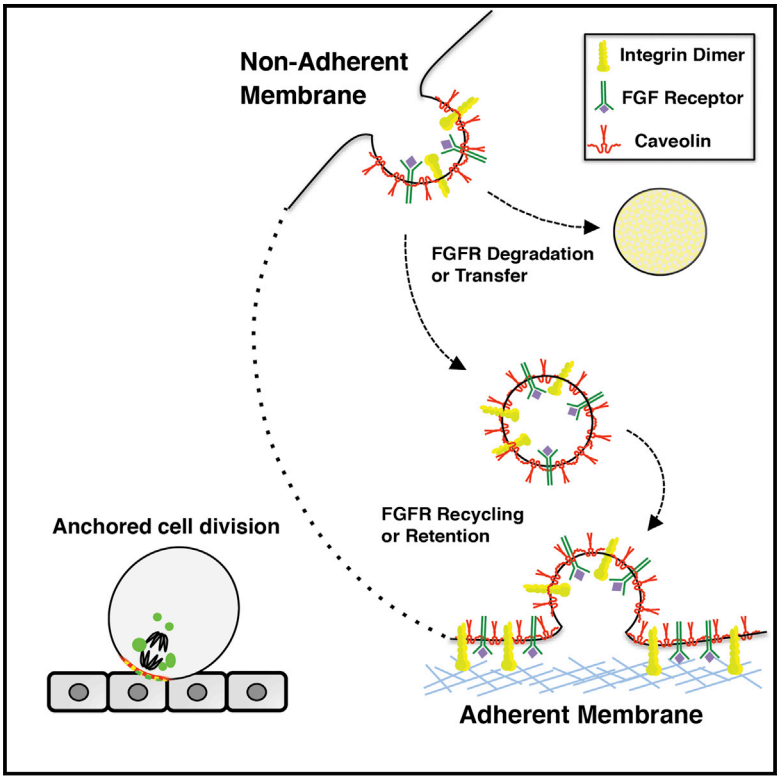

Authors

Christina D. Cota, Brad Davidson

Correspondence

bdavids1@swarthmore.edu

In Brief

In the ascidian *Ciona intestinalis*, nascent heart progenitor cells inherit an adherent membrane associated with elevated levels of FGFR signaling. Cota and Davidson now explain the basis for this observation, showing that adhesion, via effects on Caveolin-rich membrane domains, limits FGFR internalization, leading to receptor enrichment at the adherent membrane.

Highlights

- Mitotic redistribution of FGFRs promotes differential heart progenitor induction
- Polarized mitotic FGFR redistribution is dependent on matrix adhesion
- Cytoplasmic NPxX motifs govern β-integrin-specific effects on FGFR redistribution
- Caveolin functions downstream of adhesion to drive polarized FGFR distribution

Cota & Davidson, 2015, Developmental Cell *34*, 505–519
September 14, 2015
http://dx.doi.org/10.1016/j.devcel.2015.07.001

CellPress

Developmental Cell
Article

Mitotic Membrane Turnover Coordinates Differential Induction of the Heart Progenitor Lineage

Christina D. Cota[1] and Brad Davidson[1,*]
[1]Department of Biology, Swarthmore College, Swarthmore, PA 19081, USA
*Correspondence: bdavids1@swarthmore.edu
http://dx.doi.org/10.1016/j.devcel.2015.07.001

SUMMARY

In response to microenvironmental cues, embryonic cells form adhesive signaling compartments that influence survival and patterning. Dividing cells detach from the surrounding matrix and initiate extensive membrane remodeling, but the in vivo impact of mitosis on adhesion-dependent signaling remains poorly characterized. We investigate in vivo signaling dynamics using the invertebrate chordate, *Ciona intestinalis*. In *Ciona*, matrix adhesion polarizes fibroblast growth factor (FGF)-dependent heart progenitor induction. Here, we show that adhesion inhibits mitotic FGF receptor internalization, leading to receptor enrichment along adherent membranes. Targeted disruption of matrix adhesion promotes uniform FGF receptor internalization and degradation while enhanced adhesion suppresses degradation. Chimeric analysis indicates that integrin β chain-specific impacts on induction are dictated by distinct internalization motifs. We also found that matrix adhesion impacts receptor enrichment through Caveolin-rich membrane domains. These results redefine the relationship between cell division and adhesive signaling, revealing how mitotic membrane turnover orchestrates adhesion-dependent signal polarization.

INTRODUCTION

Embryonic cells interpret a complex suite of cues in order to respond appropriately to their dynamic microenvironment. Microenvironmental cues include transmembrane proteins on adjacent cells, paracrine signals, and extracellular matrix. Cells adhere to the matrix through Integrin receptors. Once bound, Integrins recruit large cytoplasmic complexes capable of integrating diverse extracellular inputs (Streuli and Akhtar, 2009; Hu and Luo, 2013; Ivaska and Heino, 2011; Moser et al., 2009). The impact of matrix adhesion on cellular information processing has been studied primarily in four contexts. In migrating cells, matrix adhesion provides mechanical traction and coordinates cell polarization including localized enrichment of chemosensory receptors (Caswell and Norman, 2008; Huttenlocher and Horwitz, 2011). In pre-cancerous cells, escape from adhesion-dependent growth regulation results in ectopic signal activation and uncontrolled proliferation (Guadamillas et al., 2011). During mitosis, matrix adhesion contributes to spindle alignment, impacting the orientation and symmetry of division (Toyoshima and Nishida, 2007). In vitro studies have also revealed that matrix adhesion can profoundly influence growth factor signaling thereby impacting stem cell fate specification (Dave et al., 2014; Engler et al., 2006; Reilly and Engler, 2010; Yim and Sheetz, 2012). In contrast, relatively few studies have focused on the role of matrix adhesion in embryonic cell specification (Miller and Davidson., 2013; Brunet et al., 2013; Farge, 2011; Fonar et al., 2011; Martin-Bermudo, 2000; Norton et al., 2013). Thus, the dynamic, in vivo impact of matrix adhesion on embryonic cell fate decisions remains poorly characterized.

The invertebrate chordate *Ciona intestinalis* represents a valuable model organism for studying the in vivo cell biology of fate specification. Due to their close phylogenetic relationship, *Ciona* and vertebrate embryos share unique, derived developmental features (Davidson, 2007; Lemaire, 2011). In comparison with their vertebrate cousins, *Ciona* embryos have greatly reduced genomic complexity (Cota et al., 2014; Dehal et al., 2002). *Ciona* embryos also develop with extremely low cell numbers, facilitating high-resolution in vivo analysis (Stolfi and Christiaen, 2012). The extreme cellular simplicity of *Ciona* embryogenesis is exemplified by the heart lineage (Figure 1A). The *Ciona* heart can be traced back to four cardiac founder cells (the B7.5 lineage; Davidson and Levine, 2003). Each bilateral founder cell pair divides asymmetrically to produce bilateral quartets containing two smaller anterior daughters and two larger posterior daughters. Within each quartet, FGF signaling differentially induces Mitogen Activated Protein Kinase (MAPK)-dependent heart progenitor specification in the smaller daughter cells (the Trunk Ventral Cells; Davidson et al., 2006). Previous work has revealed a key role for matrix adhesion in differential heart progenitor induction (Figure 1A′). Prior to division, founder cells exhibit a broad domain of matrix adhesion along the ventral, epidermal boundary (Norton et al., 2013). This adherent domain correlates with a broad region of FGF receptor activation. Invasive protrusions associated with mitosis appear to anchor the ventral founder cell membrane, preserving a restricted domain of adhesion and associated FGFR activity during mitotic rounding (Cooley et al., 2011; Norton et al., 2013). Following division, nascent heart progenitors inherit the adherent signal-enriched ventral membrane. Thus, although dividing founder cells are exposed uniformly to FGF (Cooley et al., 2011), sustained matrix

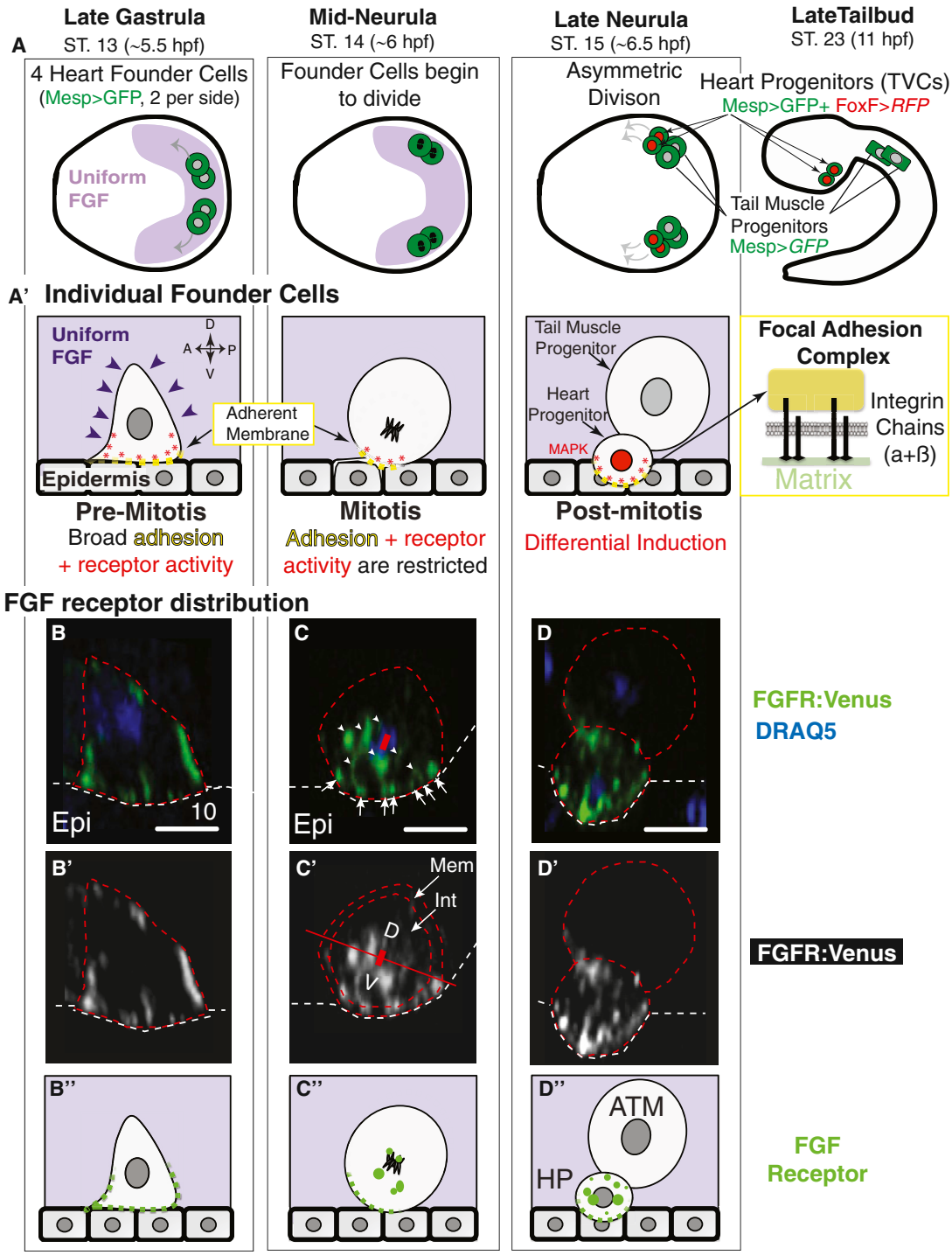

Figure 1. Polarized Distribution of FGFR:Venus during Founder Cell Division

(A) Position of cardiac founder lineage cells in *Ciona* embryos, ventral views for early stages, lateral view at stage 23.

(A′) Model of differential induction in an individual founder cell, lateral view, based on previous data (Beh et al., 2007; Cooley et al., 2011; Davidson et al., 2005; Norton et al., 2013).

(B–D′′) Lateral sections and accompanying diagrams of Mesp>*FGFR:Venus* staining in founder lineage cells (Hotta stages 13–15 as indicated at the top of each column) stained as indicated; dashed lines indicate phalloidin stained cell membranes (red) or epidermal border (white, Epi). Because phalloidin staining obscures FGFR localization, this channel is not shown. Membrane-associated (arrows) and intracellular (arrowheads) FGFR:Venus foci are indicated.

(C′) Measurements of FGFR:Venus staining along the membrane were used to determine a Ventral/Dorsal (V/D) ratio. D, dorsal; V, ventral; HP, heart progenitor; ATM, anterior tail muscle cell. Scale bars are indicated in micrometers. Embryos oriented anterior to the left.

See also Figure S1.

adhesion along the ventral membrane potentiates differential induction (Norton et al., 2013). Although we have previously demonstrated an essential role for matrix adhesion in heart progenitor induction (Norton et al., 2013), the precise molecular link between adhesion and inductive signaling has remained unresolved. Here, we provide evidence that matrix-adhesion impacts membrane dynamics, polarizing FGF receptor distribution to drive differential heart progenitor induction.

RESULTS

FGF Receptor Is Enriched along the Ventral, Adherent Membrane during Founder Cell Mitosis

We first investigated the proximal mechanism underlying differential induction in response to uniform FGF exposure. The most straightforward hypothesis for differential induction is polarized FGF receptor distribution. We therefore assayed FGFR distribution by expressing fluorescently tagged FGFR (FGFR:Venus) specifically in the *Ciona* founder cell lineage using the well-characterized Mesp enhancer (Mesp>*FGFR:Venus*; Davidson et al., 2006). To alleviate concerns regarding the potential impact of this construct on induction, we co-transfected embryos with Mesp>*GFP* and FoxF>*RFP* reporter constructs (Figures 1A and S1A). FoxF>*RFP* reporter activity within Mesp>*GFP* labeled founder lineage cells represents a well-established assay for heart progenitor specification (Figures 1A and S1A; Beh et al., 2007; Cooley et al., 2011; Norton et al., 2013). In wild-type embryos, heart progenitors express FoxF>*RFP* shortly after founder cell division (Cooley et al., 2011) and migrate anteriorly into the head (Figure S1B; Beh et al., 2007). Co-transfection with Mesp>*FGFR:Venus* had no discernable impact on induction or migration (Figure S1C). We therefore began to employ Mesp>*FGFR:Venus* to examine FGFR distribution during founder cell mitosis. Transgenic Mesp>*FGFR:Venus* embryos were collected at 15-min intervals spanning mitosis and co-stained with a chromatin marker (DRAQ5) to facilitate precise mitotic staging (Figures 1B–1D; Hotta et al., 2007). In pre-mitotic founder cells (stage 13), FGFR:Venus is enriched along both ventral and lateral membranes (Figure 1B). During mitosis (stage 14), FGFR:Venus accumulates in large intra-cellular foci (arrowheads, Figure 1C), suggesting that FGF receptors are internalized during pervasive membrane turnover characteristic of dividing cells (Boucrot and Kirchhausen, 2007; Fürthauer and González-Gaitán, 2009; McKay and Burgess, 2011; Tacheva-Grigorova et al., 2013). Notably, redistribution of FGFR in mitotic founder cells appears to be highly polarized. FGFR:Venus staining in intracellular foci or along the plasma membrane was dramatically enriched on the ventral side (V_{Total}/D_{Total} = 3.60 ± 0.63; Figure 1C′). Because signaling is terminated in more central, mature endocytic compartments (Goh and Sorkin, 2013), we focused further analysis on FGFR:Venus staining proximal to the plasma membrane. Quantitative analysis comparing fluorescence in ventral versus dorsal membrane regions confirmed consistent and significant ventral enrichment during mitosis (V_{Mem}/D_{Mem} = 4.44 ± 0.84, Figure 1C′). Consistent ventral enrichment of FGFR:Venus also occurred internally (V_{Int}/D_{Int} = 2.84 ± 0.49). Following division, FGFR is highly concentrated in the heart progenitor lineage, presumably due to differential inheritance of receptor-enriched plasma membrane or associated vesicles (Figure 1D). Thus, our data support a model in which differential induction is driven by unequal receptor distribution during founder cell mitosis.

FGF Signaling Is Not Required for Mitotic FGF Receptor Enrichment

Receptor internalization and trafficking is often modulated by ligand binding and downstream pathway activation (Goh and Sorkin, 2013). We were therefore interested in examining whether FGF signaling recursively regulates FGFR distribution. To investigate this hypothesis, we blocked FGF signaling through targeted expression of a Venus-tagged dominant-negative FGFR fusion protein (Mesp>*$FGFR^{DN}$:Venus*; Davidson et al., 2006). Previous work has shown that expression of $FGFR^{DN}$:Venus in founder cells completely blocks heart progenitor induction (Davidson et al., 2006). Analysis of $FGFR^{DN}$:Venus distribution indicated that loss of FGF signaling had no discernable impact on FGFR distribution (Figure S1). $FGFR^{DN}$:Venus was enriched along adherent membranes during mitosis and robustly partitioned in adherent daughter cells following mitosis (cf. Figures S1D–S1F to Figures 1B–1D). Intriguingly, transfection with $FGFR^{DN}$:Venus appeared to disrupt the unequal division of founder cells (Figure S1F). To verify this observation, we measured the volume of founder cell daughters in control and $FGFR^{DN}$:Venus transgenic embryos and calculated the volume ratio between the smallest and largest pairs. Control founder cells consistently divide in a highly unequal fashion, as indicated by a median volume ratio of 2.35. In contrast, $FGFR^{DN}$:Venus transgenic founder cells divide equally, with a median volume ration of 1.35 (Figure S1G). Thus, FGF signaling does not appear to impact FGFR enrichment but does play an unanticipated role in directing the plane of founder cell division. Furthermore, these data indicate that cellular anisotropies associated with unequal division (including displacement of the mitotic spindle and cytokinetic ring) are not required for polarized FGFR enrichment.

Matrix Adhesion Is Necessary and Sufficient for Mitotic FGF Receptor Enrichment

The spatiotemporal pattern of FGFR:Venus distribution mirrors the gradual constriction of matrix adhesion along the epidermal boundary previously observed during mitotic rounding (Figure 1A; Norton et al., 2013). Additionally, we previously found that regional matrix adhesion mediates differential induction (Norton et al., 2013). We therefore hypothesized that adhesion impacts mitotic FGFR distribution, promoting receptor enrichment along the presumptive heart progenitor membrane, a process we term "adhesive enrichment." To test this hypothesis, we disrupted adhesion using a dominant-negative Rap construct (Mesp>*Rap^{S17N}*) and examined the effect on FGFR:Venus localization. Rap functions as a molecular switch upstream of Integrin activation (Boettner and Van Aelst, 2009) and targeted expression of Rap^{S17N} disrupts heart progenitor induction specifically through its impact on matrix adhesion (Figure 2A; Norton et al., 2013). As previously observed, the majority of Rap^{S17N} founder cells appear completely detached, exhibiting a rounded morphology and dorsal displacement away from the epidermis (cf. Figure 2B versus Figure 2C). Occasionally, Rap^{S17N} founder cells maintain limited adhesion along the epidermal boundary,

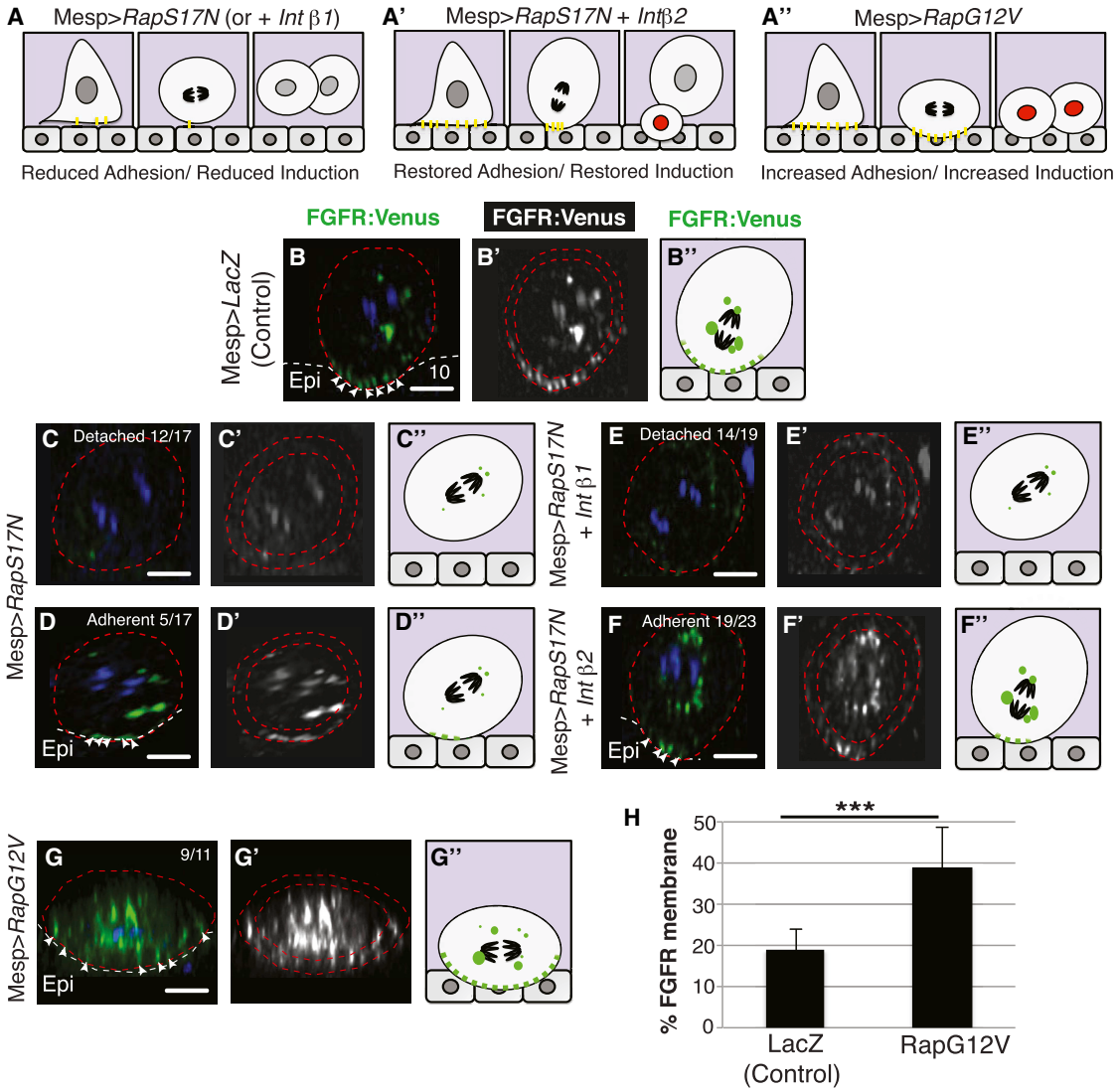

Figure 2. Matrix Adhesion Is Necessary and Sufficient for FGF Receptor Enrichment

(A–A′′) Illustrations showing (A and A′) Intβ2-specific rescue of adhesion/heart progenitor induction in transgenic Rap^{S17N} founder lineage cells and (A′′) increased adhesion and heart progenitor induction associated with constitutive Rap activation (Rap^{G12V}) based on previous data (Norton et al., 2013). Adhesive foci (yellow). Heart progenitor induction indicated by red nuclei.

(B–G′′) Lateral sections and accompanying diagrams of FGFR:Venus distribution in mitotic founder cells co-transfected as labeled. Membrane-associated FGFR:Venus foci are indicated (arrows). Dashed lines indicate phalloidin stained cell membranes (red) or epidermal border (white, Epi).

(H) Quantitation of FGFR:Venus staining along the periphery of transgenic LacZ control and Rap^{G12V} founder cells. *p = 0.0007 for LacZ versus Rap^{G12V}.

Scale bars are indicated in micrometers. Embryos are oriented anterior to the left.

resulting in less severe displacement (Figure 2D; Norton et al., 2013). In fully detached founder cells, FGFR:Venus is uniformly internalized and appears to undergo subsequent degradation during mitosis. Thus, by metaphase FGFR:Venus staining was largely absent (Figure 2C). In partially detached founder cells, FGFR:Venus was present in both intracellular foci and along persistent adherent membranes (arrows, Figure 2D). These data indicate that matrix adhesion is required for localized FGFR enrichment in dividing founder cells, possibly by inhibiting internalization or by promoting recycling. Additionally, these adhesion-dependent modifications in trafficking appear to regionally suppress FGFR degradation.

Because Rap GTPases perform multiple regulatory functions (Boettner and Van Aelst, 2009), we focused on determining whether Rap^{S17N} specifically impacts mitotic FGFR enrichment by perturbing matrix adhesion. Mirroring previous studies (Norton et al., 2013), we examined whether restoration of matrix adhesion was sufficient to rescue FGFR enrichment in a transgenic Mesp>Rap^{S17N} background. Co-expression of *Ciona* Integrin-β1 (Mesp>*Intβ1*) does not restore adhesion or induction (as illustrated in Figure 2A and Norton et al., 2013). In contrast, co-expression of another β chain, Integrin-β2 (Mesp>*Intβ2*), restores founder cell adhesion and heart progenitor induction in Mesp>Rap^{S17N} founder cells (as illustrated in Figure 2A′; Norton et al., 2013). Using

the FGFR:Venus assay, we found that Integrin-β chains have a similar, selective impact on FGFR enrichment. Mesp>*Intβ1* failed to restore receptor enrichment in transgenic Mesp>*Rap*^{S17N} founder cells (Figure 2E). Mesp>*Intβ2*, on the other hand, led to a robust and significant restoration of FGFR enrichment (arrows, Figure 2F). Strikingly, Intβ2-dependent restoration of FGFR enrichment occurs in a similar proportion of embryos (82.6% ± 1.9%, SEM) as Intβ2-dependent restoration of induction (75.8% ± 1.2%, SEM; observed previously Norton et al., 2013). Thus, rescuing matrix adhesion is sufficient to restore localized FGFR enrichment and differential induction.

We further examined the proposed sufficiency of matrix adhesion in FGFR enrichment by transfecting embryos with a constitutively active Rap construct, Mesp>*Rap*^{G12V} and examining the impact on FGFR:Venus distribution. Previously, we have shown that expression of Rap^{G12V} in cardiac founder cells results in enhanced matrix adhesion and increased heart progenitor induction (as illustrated in Figure 2A″; Norton et al., 2013). During mitosis, Mesp>*Rap*^{G12V} transgenic founder cells are flattened along the ventral epidermal boundary, presumably reflecting their increased adhesion to the epidermal matrix (cf. Figure 2G to Figure 2B). Increased adhesion is mirrored by a dramatic and significant enhancement of FGFR:Venus staining both internally and along the expanded adherent ventral membrane (cf. Figure 2G′ to Figure 2B′). In mitotic control cells, FGFR:Venus is associated with the plasma membrane along approximately 19% of the founder cell periphery (Figures 2B′ and 2H). In mitotic Rap^{G12V} cells, FGFR:Venus is associated with the membrane along ~40% of the founder cell periphery (Figures 2G′ and 2H). In post-mitotic Rap^{G12V} cells, FGFR:Venus is present in both daughter cells (data not shown). Taken together, these data show that matrix adhesion is both necessary and sufficient for localized FGFR enrichment, strongly supporting the core premise of our "adhesive enrichment" model.

Selective Restoration of FGF Receptor Enrichment by Integrin-β2

We next began to explore the adhesive enrichment model through comparative, functional analysis of *Ciona* Integrin-β chains. Integrin β1 and β2 are highly divergent proteins with distinct N-terminal extracellular domains conferring matrix binding specificity and distinct C-terminal cytoplasmic domains conferring discrete signal transduction properties (Liu et al., 2000). Because Integrin β2 selectively inhibits mitotic FGF receptor internalization, we hypothesized that β2-specific domains regulating internalization would be more relevant than either matrix binding or signal transduction domains. In particular, we focused on conserved variations within well-characterized C-terminal NPxX motifs (Figures 3A and 3B; Caswell et al., 2009; Moser et al., 2009). Previous studies suggest that NPxY phosphorylation regulates integrin activity and trafficking (Anthis et al., 2009; Pellinen et al., 2008). Clathrin adaptors, including DAB and NUMB, bind NPxX motifs to regulate Integrin endocytosis (Nishimura and Kaibuchi, 2007; Teckchandani et al., 2009). In β1 family Integrins, the distal motif includes a tyrosine (NPxY), while in β2 family Integrins it does not (NPxF; Figures 3A and 3B; Calderwood et al., 2003). Replacement of Intβ1 NPxX tyrosine residues with phenylalanines (β1^{YYFF}) decreased endocytosis and inhibited focal adhesion turnover (Pellinen et al., 2008). We reasoned that selective restoration of induction by Intβ2 in Rap^{S17N} founder cells might reflect decreased internalization of adherent membranes conferred by the absence of tyrosine residues in the β2 tail motif (Figure 3A). To test this hypothesis, we introduced a Y>F amino acid substitution into the distal NPxY motif of the Integrin-β1 cytoplasmic tail, rendering this motif non-phosphorylatable (Mesp>*Intβ1*^{Y694F}; Figure 3B). We also introduced the reciprocal F>Y substitution in Integrin-β2 (Mesp>*Intβ2*^{F801Y}; Figure 3B). The mutated β chain constructs were then co-transfected with Mesp>*Rap*^{S17N} and FoxF>*RFP*. Remarkably, these single amino acid substitutions were sufficient to completely reverse β chain-specific restoration of heart progenitor induction. Co-expression of non-phosphorylatable Intβ1^{Y694F} rescued heart progenitor induction; producing results indistinguishable from those observed for Mesp>*Intβ2* (Figures 3D–3F and 3J; Figure S2). Conversely, co-transfection with phosphorylatable Intβ2^{F801Y} failed to rescue induction, producing results indistinguishable from those observed for Mesp>*Intβ1* (Figures 3G–3J; Figure S2). We also tested whether mutated β chain constructs were able to restore matrix adhesion, using an established ex vivo assay (Norton et al., 2013). Consistent with the presumed impact on mitotic internalization; introduced mutations reversed β chain-specific restoration of heart progenitor adhesion. Expression of Intβ1^{Y694F} restored heart progenitor adhesion in cells co-transfected with Mesp>*Rap*^{S17N}; producing results similar to those observed for Mesp>*Intβ2* (cf. Figure 3C to Figure 6E and Norton et al., 2013). Conversely, co-transfection with Intβ2^{F801Y} failed to restore adhesion, producing results similar to those observed for Mesp>*Intβ1* (Figure 3C; Norton et al., 2013).

Molecular crosstalk between Integrins and growth factor signaling occurs on multiple levels. Integrin-dependent remodeling of the extracellular matrix can impact the distribution and availability of ligands including FGF (Kim et al., 2011). Integrin and growth factor receptor complexes also activate overlapping cytoplasmic signal cascades (Legate et al., 2009). Furthermore, Integrin activation promotes local changes in plasma membrane composition and underlying cortical domains thereby impacting growth factor receptor trafficking and/or compartmentalization (Ivaska and Heino, 2011). Our mutational analysis demonstrates that β chain-specific impacts on induction arise solely from differences in the cytoplasmic NPxX motif. Thus, β chain-specific matrix binding or cytoplasmic signaling properties do not account for the observed differences in their inductive potential. Along these lines, targeted expression of constructs designed to disrupt Integrin-dependent signal transduction (Delcommenne et al., 1998; Shibue and Weinberg, 2009), including dominant-negative Integrin-linked Kinase (Mesp>*ILK*^{DN}) or Focal Adhesion Kinase (Mesp>*FRNK*), had no impact on heart progenitor induction (data not shown). Taken together, these results suggest that adhesion primarily impacts heart progenitor induction by altering membrane dynamics, suppressing mitotic internalization of FGFR-enriched membranes and subsequent degradation.

FGF Receptor Enrichment and Heart Progenitor Induction Are Increased by Perturbing Receptor Degradation

To begin investigating the proposed role of degradation in adhesion-dependent FGFR enrichment, we attempted to perturb the

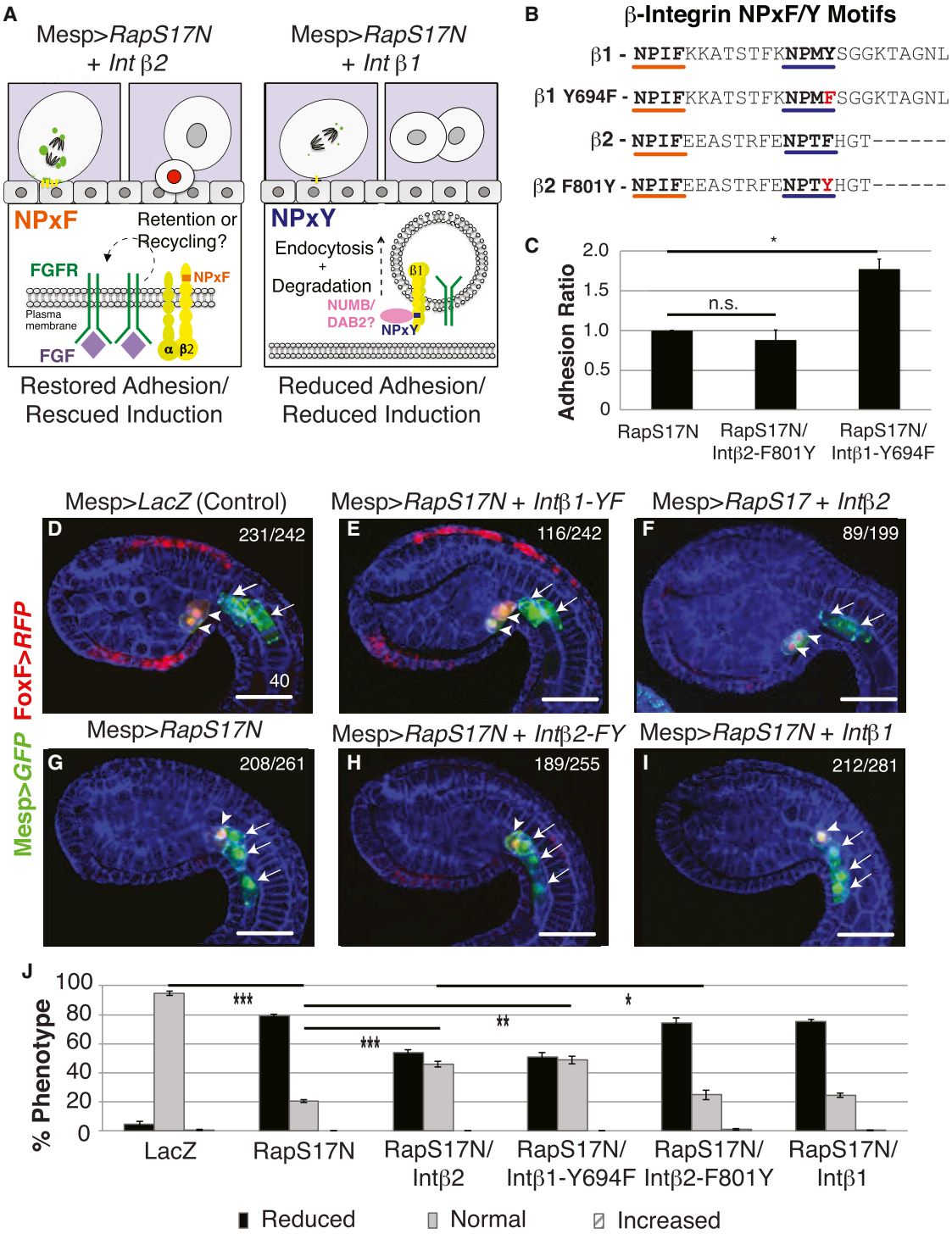

Figure 3. Selective Restoration of FGF Receptor Enrichment by Intβ2 Is Dependent on Conserved NPxF Motif

(A) Proposed model for Intβ2-specific rescue of founder cell adhesion and heart progenitor induction.

(B) ClustalW alignment of *C. intestinalis* Intβ1 and Intβ2 cytoplasmic tail domains. Proximal NPxF motifs (orange) and distal NPxY/F motifs (blue) as well as amino acid substitutions (red) are indicated.

(C) Adhesion ratio of dissociated transgenic founder cells plated on Fibronectin (normalized to mean levels of adhesion in Rap^{S17N} cells). Data were obtained from three independent trials. *p = 0.236 (n.s.) for LacZ versus $Intβ2^{F801Y}$, 0.013 for LacZ versus $Intβ1^{Y694F}$ and 0.002 for $Intβ2^{F801Y}$ versus $Intβ1^{Y694F}$.

(D–I) Representative micrographs showing heart progenitor induction (FoxF>*RFP*, arrowheads) versus non-induced founder lineage cells (Mesp>*GFP* alone, arrows) in embryos co-transfected as indicated.

(legend continued on next page)

degradation pathway and examine the impact on FGFR:Venus distribution. Previous studies have demonstrated that application of the proteasome inhibitor MG132 provides a crude but effective strategy for inhibiting FGFR degradation (Bonaventure et al., 2007; Hatch et al., 2006; Kaabeche et al., 2004; Monsonego-Ornan et al., 2002). We therefore treated transgenic embryos (Mesp>*Rap*^{S17N}, Mesp>*FGFR:Venus*, + Mesp>*LacZ*) with MG132 or with the carrier solution (DMSO) for 1 hr prior to the onset of founder cell division and examined FGFR:Venus staining. The majority of DMSO treated Rap^{S17N} founder cells displayed a complete loss of FGFR:Venus staining (Figures 4A and 4C). MG132 treatment dramatically reversed this trend, significantly increasing the proportion of FGFR:Venus positive founder cells in Rap^{S17N} transgenic embryos (Figures 4B and 4C). In addition, we found that MG132-treatment restored normal heart progenitor induction in a significant proportion of Mesp>*Rap*^{S17N} transgenic embryos (Figure 4D; Figures S3A–S3D). Furthermore, MG132 treatment of Mesp>*LacZ* control embryos was sufficient to generate a small but significant proportion of embryos displaying enhanced induction (Figure 4D). These results suggest that differential heart progenitor induction involves regional, adhesion-dependent suppression of FGFR degradation.

Correlation between Caveolin and FGFR Distribution during Founder Cell Mitosis

To further investigate the molecular link between adhesion and mitotic membrane turnover, we focused our analysis on Caveolin. Caveolins are integral membrane proteins that modulate plasma membrane compartmentalization, curvature, and internalization (Parton and del Pozo, 2013). Published microarray data indicate that the *Ciona* Caveolin-1 ortholog, *Ci-CavA* (referred to hereafter as *Caveolin*), is highly expressed in founder lineage cells (Woznica et al., 2012). Caveolin-rich membrane domains (CRMs) function as scaffolds for signaling complexes (Parton and del Pozo, 2013; Zhou et al., 2014). Although CRMs have not been explicitly linked to FGF receptor trafficking, previous studies have documented Caveolin-regulated trafficking of related growth factor receptors (Di Guglielmo et al., 2003; Strålfors, 2012). Adhesion complexes are also known to inhibit CRM internalization (del Pozo et al., 2004; Strålfors, 2012). Thus, it has been proposed that adhesive maintenance of Caveolin-associated signaling domains underlies anchorage-dependent growth (Di Guglielmo et al., 2003; Du et al., 2011; Guadamillas et al., 2011; Schmidt-Glenewinkel et al., 2012). These findings prompted us to explore whether Caveolin contributes to adhesion-mediated enrichment of FGFR.

We first examined whether there is any correlation between the localization of CRM domains and FGFR during mitosis. To monitor CRM distribution, we expressed a Caveolin:GFP fusion protein in founder cells using the Mesp driver (Mesp> *Caveolin:GFP*) and examined staged embryos spanning founder cell mitosis. In pre-mitotic founder cells, Caveolin:GFP is heavily enriched along the ventral founder cell membrane (Figure 4E). Consistent with studies in mammalian epithelial cell lines (Boucrot et al., 2011; del Pozo et al., 2005), the majority of Caveolin:GFP appears to be internalized during mitosis (Figure 4F). However, as observed with FGFR:Venus, both membrane-associated and intracellular Caveolin:GFP is differentially enriched on the ventral side of dividing heart founder cells (Figure 4F). Quantification of membrane-associated Caveolin:GFP fluorescence confirms that the observed ventral enrichment is consistent and significant (V_{Mem}/D_{Mem} = 2.83 ± 0.43, V_{Int}/D_{Int} = 2.62 ± 0.10; Figure 4F′). After division, Caveolin:GFP is highly concentrated in the newly formed heart progenitors (Figure 4G). Thus, Caveolin:GFP and FGFR:Venus share similar distribution patterns (cf. Figures 1 and 4). To better evaluate the apparent confluence between Caveolin and FGFR localization patterns in mitotic founder cells, we generated transgenic embryos co-expressing FGFR:Venus and Caveolin:RFP. In these double transgenic founder cells, a partially overlapping distribution pattern along the ventral, adherent membrane was evident (Figures S3H and S3I).

Matrix Adhesion Is Required for Mitotic Caveolin Distribution

We next examined whether matrix adhesion is required for maintenance of CRMs during founder cell mitosis. For this purpose, we inhibited matrix adhesion through targeted expression of Rap^{S17N} and examined the impact on Caveolin:GFP distribution. Disrupting adhesion had a dramatic impact on Caveolin:GFP distribution (Figures 4H, 4I, S3F, and S3G). In fully detached mitotic founder cells, Caveolin:GFP membrane enrichment was abrogated, replaced by staining in intracellular foci (Figure 4I). In partially detached founder cells, Caveolin:GFP staining persisted along adherent membranes (Figure 4H). Thus it appears that Caveolin:GFP internalization during mitosis is inhibited along adherent membranes, mirroring the pattern observed for FGFR:Venus (Figures 1B–1D). These results indicate that localized matrix adhesion promotes mitotic retention of CRMs (Figures 4J and 4J′), in accordance with published observations in mammalian cells (del Pozo et al., 2005).

Caveolin-Rich Membrane Domains Are Required for FGFR Enrichment and Heart Progenitor Induction

We next focused on determining whether CRMs are required for differential, mitotic FGFR enrichment. For this purpose, we carried out targeted mutagenesis of *Ciona Caveolin* (*CavA*) using a tissue-specific CRISPR/Cas9 expression construct (Stolfi et al., 2014). Guide RNAs targeting exon 1 of *Caveolin* (Figure 5C) were cloned into the previously characterized *Ciona* U6>*sgRNA(F+E)* vector (U6>*CavA.39 gRNA*, Table S1; Stolfi et al., 2014). To control for potential off-target effects, we introduced single base mismatches in the U6>*CavA.sgRNA* constructs (Table S1; Sasaki et al., 2014). To assay their impact on

(G–I) Data were obtained from three independent trials, n > 31/trial. p values comparing percentage of normal induction, *p = 0.0002 for LacZ versus Rap^{S17N}, 0.001 for Rap^{S17N} versus Intβ2, 0.003 for Rap^{S17N} versus Intβ1^{Y694F} and 0.013 for Intβ2 versus Intβ2^{F801Y}. Error bars represent the SEM in (C) and (J).
(J) Quantitative analysis of induction data. Two of four FoxF>*RFP* positive founder lineage cells was scored as "normal induction" (D–F). Less than two FoxF>*RFP* positive cells was scored as "reduced induction."
Significance was determined using a two-tailed unpaired t test. Scale bars are indicated in micrometers. Embryos oriented anterior to the left. See also Figure S2.

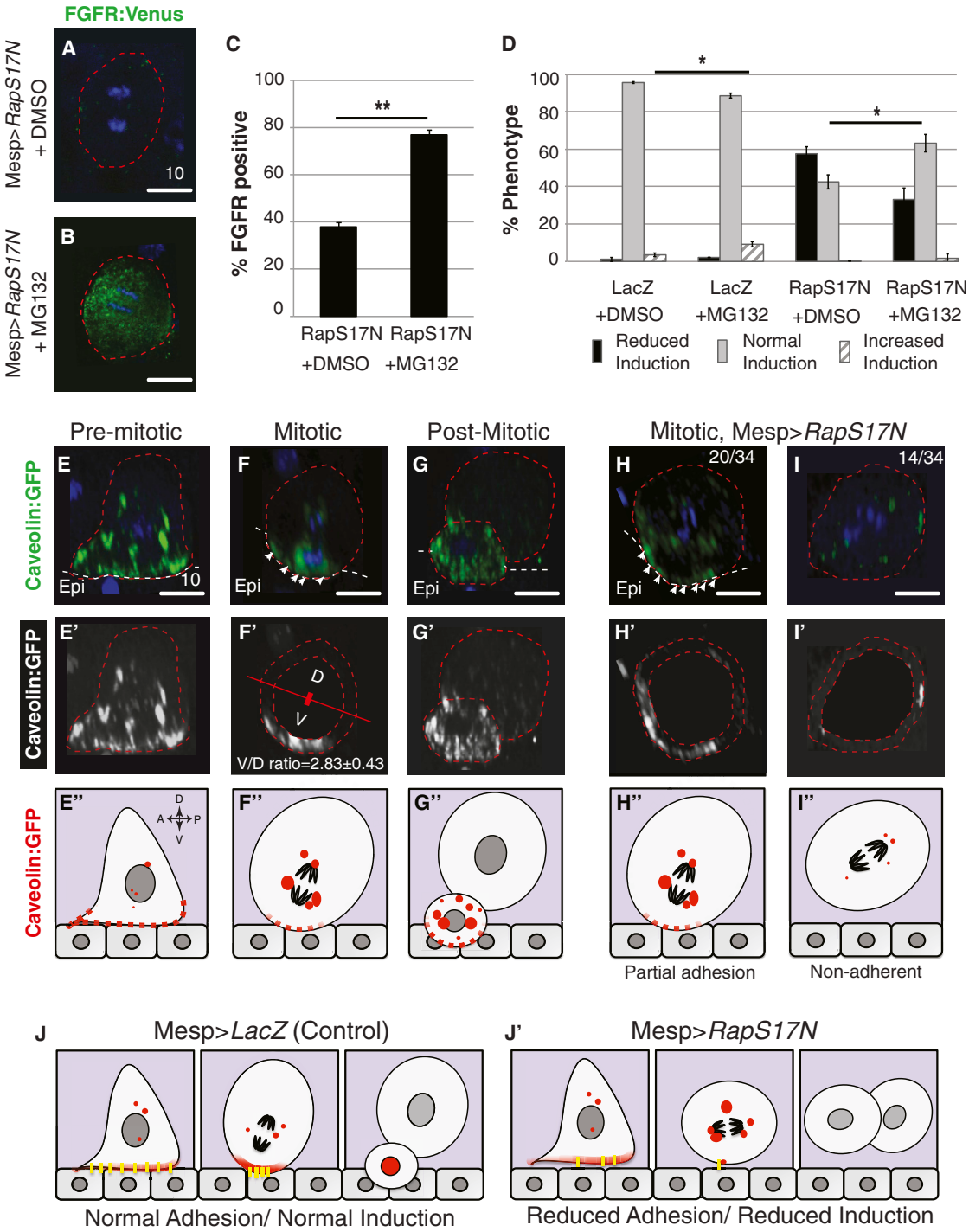

Figure 4. Matrix Adhesion Is Required for Mitotic CRM Enrichment during Heart Progenitor Induction

(A–C) Lateral sections showing representative FGFR:Venus staining in Rap^{S17N} transgenic founder cells treated with DMSO (A) or MG132 (B) and graphical summary (C) of FGFR staining in LacZ control and Rap^{S17N} transgenic founder cells treated as indicated. Data were obtained from two independent trials, n > 44/trial. *p = 0.005.

(D) Graphical summary of induction data. Data were obtained from three independent trials, n > 29/trial. Error bars represent the SEM. *p = 0.030 for increased induction in LacZ+DMSO versus LacZ+MG132 and 0.037 for normal induction in Rap^{S17N}+DMSO versus Rap^{S17N}+MG132. Significance was determined using a two-tailed unpaired t test in (C and D).

(E–I'') Lateral sections and accompanying diagrams of Mesp>*Caveolin:GFP* distribution in mitotic founder cells co-transfected as labeled. Dashed lines indicate phalloidin stained cell membranes (red) or epidermal border (white, Epi). Membrane-associated Caveolin:GFP foci are indicated (arrows).

(legend continued on next page)

FGFR trafficking, *Caveolin* gRNAs were co-electroporated with Mesp>*nls::Cas9::nls* and Mesp>*FGFR:Venus*. FGFR distribution in mitotic founder cells co-transfected with the mismatch control construct (Mesp>*nls::Cas9::nls* + U6>*CavA.39 gRNAmm2*) appeared identical to control embryos, displaying clear FGFR enrichment along the ventral membrane (cf. Figure 5A to Figure 1C). In contrast, co-transfection with the matching sgRNA (Mesp>*nls::Cas9::nls* + U6>*CavA.39 gRNA*) abrogated polarized FGFR:Venus enrichment in 31.3% of mitotic founder cells (Figure 5B). To verify that the observed defects in FGFR trafficking were associated with mutagenesis of *Caveolin*, we amplified and sequenced the presumed CRISPR target region in exon 1. In transgenic embryonic samples, mutations specific to the targeted region occurred in 25% (2/8) of exonic sequences (Figure 5D). We also investigated the impact of Caveolin knockdown on differential heart progenitor induction. In CRISPR mismatch controls (Mesp>*nls::Cas9::nls* + U6>*CavA.39 gRNAmm*), we consistently observed the wild-type induction pattern (Figures 5E, 5G, and S4C) at levels indistinguishable from typical loading controls (cf. Figures 5E and 5G to Figures 3D and 3J). In contrast, 19% of transgenic Mesp>*nls::Cas9::nls* + U6>*CavA.39 gRNA* embryos displayed reduced induction ($p < 0.0002$ and $p < 0.044$; Figures 5F, 5G, and S4D). Our sequence analysis (Figure 5D) indicates that low penetrance of the reduced induction phenotype associated with Caveolin CRISPR may be due to limited mutagenesis, perhaps reflecting the extremely short window (~1.5 hr) between the initial onset of Mesp-driven Cas9 expression and FGF-dependent heart progenitor induction. To produce a more robust disruption of Caveolin-enriched membranes, we also employed a dominant-negative approach. This involved targeted expression of the P189L Caveolin mutant (Mesp>*Caveolin^{P189L}:GFP*). *Ciona* Caveolin^{P189L} is analogous to human Caveolin 1^{P132L}, a mutation that disrupts CRM formation by sequestering endogenous Caveolin in the Golgi body (Lee et al., 2002; Shatz et al., 2010). We first assayed the impact of Caveolin^{P189L} on FGFR distribution through co-transfection with Mesp>*FGFR:Venus*. In control mitotic founder cells, we consistently observed the wild-type enrichment pattern (Figure S3I). In contrast, Caveolin^{P189L} expression abrogated ventral FGFR enrichment (Figure S3K). We next assayed the impact of Caveolin^{P189L} on heart progenitor induction. Mesp>Caveolin:GFP control embryos consistently displayed the wild-type induction pattern (Figures 5H, 5J, and S4E). Strikingly, over 75% of Mesp>*Caveolin^{P189L}:GFP* transgenic embryos displayed complete loss of induction, as evidenced by the absence of FoxF>*RFP* and associated heart progenitor migration (Figures 5I, 5J, and S4F). The severe impact of dominant-negative Caveolin on induction closely parallels the levels of reduced induction seen upon disruption of matrix adhesion (Mesp>*Rap^{S17N}*; Figure 3J; Norton et al., 2013). Taken together, these results indicate that Caveolin is required for localized FGFR enrichment within adherent membranes (Figures 5K and 5K′). However, they do not address whether Caveolin functions upstream or downstream of adhesion.

Caveolin-Rich Membrane Domains Promote Differential Induction Downstream of Adhesion

To begin investigating the epistatic relationship between matrix adhesion and CRMs, we expressed Caveolin (Mesp>*Caveolin:GFP*) in founder cells co-transfected with Mesp>*Rap^{S17N}*. Targeted Rap^{S17N} does not completely disrupt matrix adhesion, as illustrated by the maintenance of partial attachment in some Rap^{S17N} founder cells (Figure 2D; Norton et al., 2013). Therefore, transgenic Rap^{S17N} founder cells provide a sensitized background to explore adhesive founder cell polarization. Remarkably, co-transfection with Mesp>*Caveolin:GFP* generated a consistent and significant rescue of heart progenitor induction (Figures 6A–6D and S5). This result suggests that residual adhesion in Rap^{S17N} transgenic founder cells is sufficient for mitotic recruitment or retention of overexpressed Caveolin, thereby restoring differential induction (Figures 6F and 6F′). We were intrigued to find that rescued FoxF>*RFP* positive heart progenitors remained in the tail region, adjacent to their sister cells (arrowheads, Figure 6C). The apparent lack of heart progenitor migration in these assays suggested that Caveolin expression restored induction while failing to replenish matrix adhesion. We examined this hypothesis directly by measuring matrix adhesion of dissociated founder cells. As previously demonstrated (Norton et al., 2013), co-expression of Intβ2 re-establishes matrix adhesion in the Rap^{S17N} background (Figure 6E). Co-expression of Caveolin:GFP, on the other hand, had no impact on founder cell adhesion (Figure 6E). Thus, targeted expression of Caveolin is sufficient to restore inductive signaling even when matrix adhesion is compromised. Taken together, these results indicate that CRMs function downstream of adhesion to polarize mitotic FGFR distribution and inductive signaling.

DISCUSSION

A Revised Model for Polarized Heart Progenitor Induction in *Ciona*

Collectively, our data support a revised model for heart progenitor induction (Figure 7). According to this model, invasive founder cell protrusions promote adhesive anchoring along the underlying epidermis. Anchored adhesions are differentially maintained during mitotic rounding (Figure 7C; Cooley et al., 2011; Norton et al., 2013). Within anchored membranes, Integrin complexes promote retention of Caveolin-rich membrane domains and associated FGF receptors during mitotic membrane turnover (Figure 7C′). Retention may reflect either decreased endocytosis or increased recycling of FGFR-enriched membranes. Within non-adherent membranes, CRMs and FGF receptors are internalized and either degraded or trafficked toward the adherent membrane (Figure 7C″). Subsequently, FGFR-enriched adherent membranes or associated vesicles are inherited by heart progenitor cells, driving differential induction (Figure 7D). Our revised model has implications regarding the roles of adhesion, Caveolin and mitotic membrane turnover in receptor

(J and J′) Proposed model for adhesion-dependent enrichment of Caveolin and heart progenitor induction in LacZ and Rap^{S17N} transgenic founder cells based on current results and previous data (Norton et al., 2013). Adhesive foci (yellow), CRMs (red). Heart progenitor induction indicated by red nuclei. HP, heart progenitor; ATM, anterior tail muscle cell. Scale bars are indicated in micrometers. Embryos are oriented anterior to the left. Embryos oriented anterior to the left.
See also Figure S3.

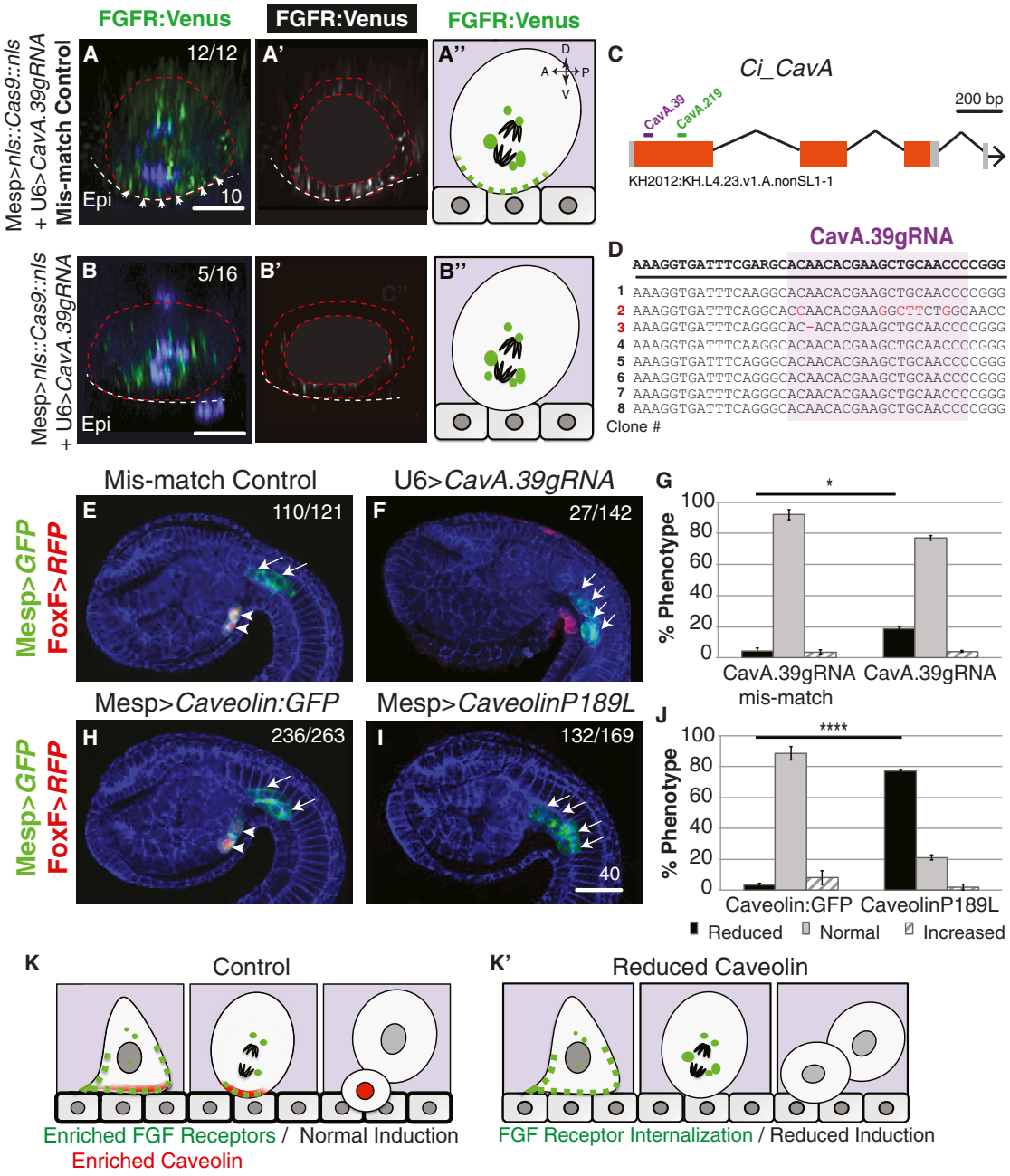

Figure 5. Caveolin Is Necessary for Mitotic FGFR Retention and Heart Progenitor Induction

(A–B″) Lateral sections and accompanying diagrams of FGFR:Venus distribution in mitotic founder cells co-transfected as labeled. Membrane-associated FGFR:Venus foci are indicated (arrows). Dashed lines indicate phalloidin stained cell membranes (red) or epidermal border (white, Epi).

(C) *Ciona intestinalis CavA* gene, showing exons (solid boxes) and introns. Approximate locations of gRNA target sequences in exon 1 are indicated.

(D) Alignment of *CavA* alleles cloned from pooled embryos electroporated with Mesp>*nls::Cas9::nls* and U6>*CavA.39 gRNA*.

(E, F, H, and I) Representative micrographs showing heart progenitor induction (*FoxF>RFP*, arrowheads) versus non-induced founder lineage cells (Mesp>*GFP* alone, arrows) in embryos co-transfected as indicated.

(G) Graphical summary of CRISPR/CAS9 induction data. Data were obtained from two independent trials, n > 41/trial. Error bars represent the SEM. *p = 0.044 for U6>*CavA.39sgRNA* mismatch (control) versus U6>*CavA.39sgRNA*.

(J) Graphical summary of Caveolin^{P189L} (dominant-negative) induction data. Data were obtained from three independent trials, n > 25/trial. Error bars represent the SEM. *p = 0.000007 for Caveolin:GFP versus Caveolin^{P189L}. Significance was determined using a two-tailed unpaired t test.

(K and K′) Proposed model for CRM-dependent FGFR enrichment and differential heart progenitor induction in control and Caveolin-deficient transgenic founder cells. CRMs (red); FGFRs (green). Heart progenitor induction is indicated by red nuclei. HP, heart progenitor; ATM, anterior tail muscle cell; Epi, ventral epidermis. Scale bars are indicated in micrometers. Embryos oriented anterior to the left. See also Figure S4.

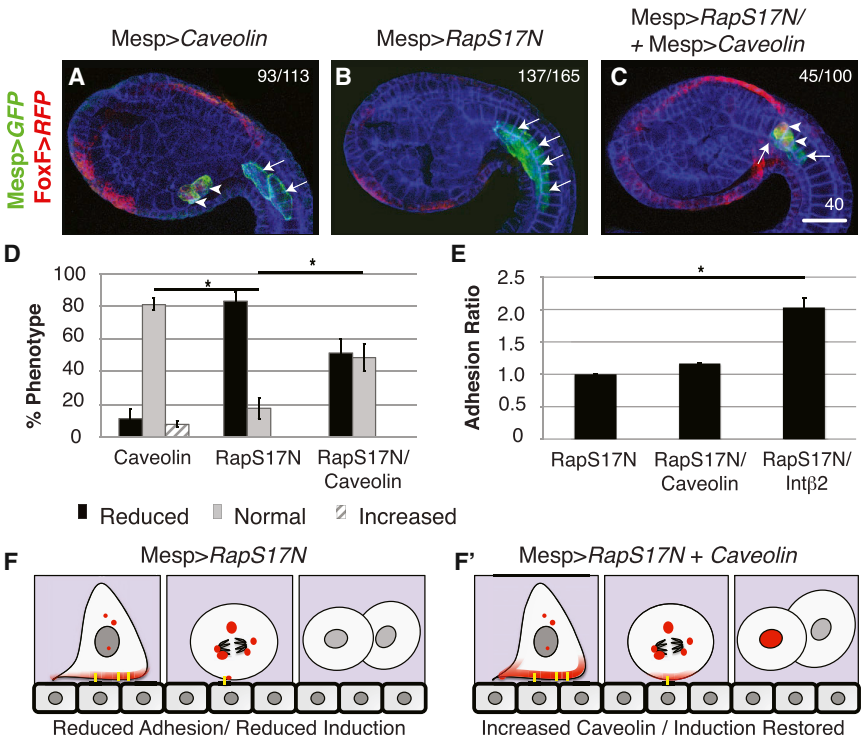

Figure 6. Caveolin Functions Downstream of Adhesion during Heart Progenitor Induction

(A–C) Representative micrographs showing heart progenitors (FoxF>*RFP*, arrowheads) versus non-induced founder lineage cells (Mesp>*GFP* alone, arrows) in embryos co-transfected as indicated.

(D) Graphical summary of induction data. Data were obtained from three independent trials, n > 22/trial. *p = 0.003 for LacZ versus Rap^{S17N} and 0.040 for Rap^{S17N} versus Caveolin:GFP.

(E) Adhesion ratio of dissociated transgenic founder cells plated on Fibronectin. Data were obtained from two independent trials. *p = 0.021 for Rap^{S17N} versus Intβ2. Error bars represent the SEM in (D) and (E). Significance was determined using a two-tailed unpaired t test.

(F and F′) Proposed model for Caveolin-dependent rescue of differential heart progenitor induction in Rap^{S17N} deficient transgenic founder cells. Residual adhesive foci are indicated (yellow bars); CRMs (red). Heart progenitor induction is indicated by red nuclei.

HP, heart progenitor; ATM, anterior tail muscle cell. Scale bars are indicated in micrometers. Embryos oriented anterior to the left. See also Figure S5.

trafficking, anchorage-dependent growth and asymmetric fate specification as discussed below.

Caveolin-Dependent Modulation of Receptor Trafficking

Our findings coincide with previous observations regarding potential contributions of CRMs to FGFR trafficking. In zebrafish embryos, ubiquitin-dependent co-localization of Caveolin and FGFR1 is associated with formation of FGF morphogen gradients (Nowak et al., 2011). In addition, Bryant et al. demonstrated that phosphorylated FGFR2 localizes to Caveolin-rich membrane fractions in oligodendrocytes and that this localization is necessary for the activation of downstream signaling (Bryant et al., 2009). Our results indicate that CRMs also suppress the mitotic turnover of FGF receptors in *Ciona* cardiac founder lineage cells. However, the precise impact of CRMs on receptor trafficking remains poorly delineated. A more refined model requires characterization of relevant CRM-dependent effectors. Further analysis will also focus on determining whether CRMs suppress FGFR turnover by inhibiting endocytosis or facilitating recycling. In addition, we intend to investigate whether CRMs modulate FGFR trafficking primarily through Clathrin-dependent or independent pathways. Furthermore, our previous research indicates that cytoskeletal dynamics associated with invasive protrusions are associated with differential induction. We are therefore interested in exploring the potential interplay between invasive protrusions, CRMs and mitotic receptor turnover. Ultimately, high-resolution in vivo analysis will be required to address many of these questions, delineating how CRM-dependent alterations of lipid composition, vesicle trafficking, and cytoskeletal dynamics are integrated to promote polarized FGFR distribution.

Differential Induction through Adhesion-Dependent Partitioning of Caveolar Signaling Domains

Our findings illustrate how three established properties of adhesive membrane organization can synergize in an unanticipated manner to promote differential induction. First, Integrins are known to modulate trafficking of Receptor Tyrosine Kinases (RTKs) and other growth factor receptors (Ivaska and Heino, 2011). Second, CRM-dependent compartmentalization of signaling pathway components is well established (Harvey and Calaghan, 2012; Patel et al., 2008). Third, multiple studies have characterized adhesion-dependent suppression of Caveolin turnover (del Pozo et al., 2004; Radel and Rizzo, 2005; Singh et al., 2007; Wickström et al., 2010). Indeed, CRM internalization is considered central to anchorage-dependent growth, ensuring termination of signaling in detached cells (Cerezo et al., 2009; del Pozo et al., 2005; Salanueva et al., 2007). These three properties are not considered specialized, cell-type-specific aspects of adhesive membrane dynamics. Rather, they are thought to reflect fundamental cellular processes. Thus, the adhesion-dependent polarization of caveolar signaling domains central to our model may represent a widespread mechanism for differential induction.

Mitosis as an Orchestrator of Adhesive Signal Compartmentalization

Our revised model also suggests that membrane turnover, an inherent property of cell division, can orchestrate differential induction. During mitosis, dramatic changes in surface area are driven by regional alterations in membrane trafficking (Boucrot and Kirchhausen, 2007; Montagnac et al., 2008). Shifts in endocytic recycling rates promote initial membrane uptake and subsequent re-distribution during anaphase and cytokinesis

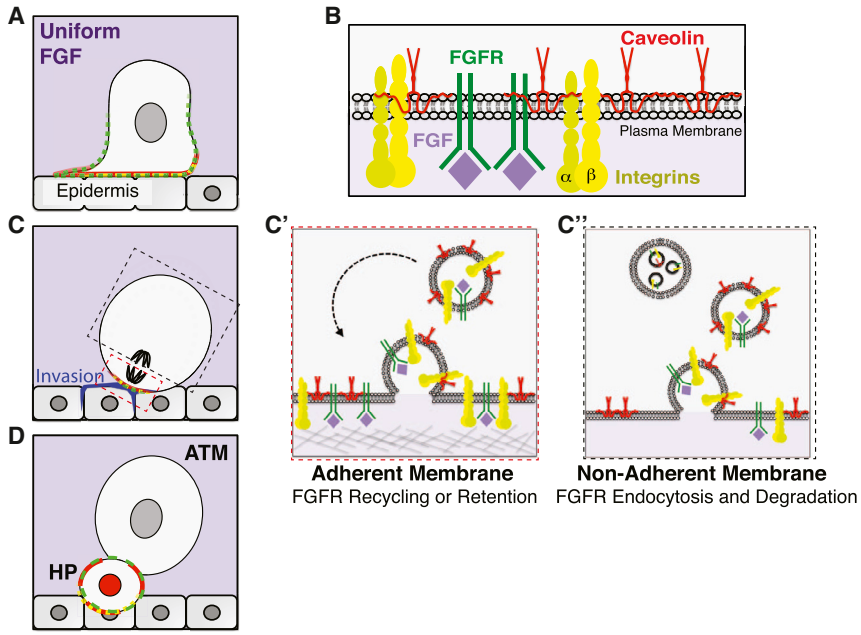

Figure 7. Revised Model of Adhesion-Dependent Heart Progenitor Induction

(A–D) Diagrams illustrating adhesion-dependent variation in receptor enrichment and trafficking during founder cell mitosis. See also Figure S6.

(Boucrot and Kirchhausen, 2007). A recent study highlighted the role of mitotic membrane turnover in re-establishing planar cell polarity (Shrestha et al., 2015). Additionally, mitotic membrane turnover encompasses Caveolin-rich domains. Caveolin-enriched vesicles are internalized during mitotic rounding and recycled back to the plasma membrane during cytokinesis (Boucrot et al., 2011). Mitotic CRM redistribution in symmetrically dividing cells is thought to ensure uniform distribution of Caveolin and associated signaling domains (Figure S6A′; Boucrot et al., 2011). Our data indicate that regionalized adhesion can break the inherent symmetry of mitotic Caveolin trafficking, resulting in polarized CRM distribution (Figure S6A″). Because CRMs facilitate receptor enrichment, mitotic CRM polarization drives asymmetric fate specification.

Our model also highlights an unanticipated, regulatory role for mitosis in adhesive signaling. According to current paradigms, mitosis is considered a regulatory target, modified by upstream asymmetries in adhesion (LaFlamme et al., 2008; Streuli, 2009). For example, stem cell niche adhesion regulates mitotic spindle orientation. The resulting shift in division plane indirectly regulates signal polarization by orienting cells within the niche (Goulas et al., 2012; Yamashita et al., 2010). Our findings shift this perspective, indicating that mitosis plays a direct, regulatory role in adhesion-dependent signal polarization. According to our model, the majority of adhesive foci are disassembled during mitotic rounding, leaving behind a regionally enriched adhesive domain. Subsequently, mitotic membrane mobilization redistributes CRM signaling platforms in accordance with newly established adhesive polarity (Figure S6). Thus, mitotic rounding functions as a threshold filter, promoting signal polarization by removing weak adhesions and thereby attenuating uniform adhesive "noise." Mitotic membrane mobilization may also function as an amplifier, enhancing polarized adhesive signaling through biased re-distribution of Caveolin-rich membrane compartments. According to this paradigm, mitosis and adhesive signaling participate in a feedback loop that may coordinate asymmetric outcomes during embryonic patterning and stem cell division.

EXPERIMENTAL PROCEDURES

Embryonic Techniques

Ciona intestinalis were supplied by M-Rep. Fertilization, staging, dechorionation, and electroporation were carried out as previously described (Cooley et al., 2011; Corbo et al., 1997).

Molecular Cloning

The *Ci-Mesp* and *FoxF* enhancers were described previously (Beh et al., 2007; Davidson et al., 2005). The Rap^{S17N}, Intβ1 and Intβ2 constructs were described previously (Norton et al., 2013). The Mesp>*Intβ1*^{Y694F} and Mesp>*Intβ2*^{F801Y} mutant constructs were generated by site-directed mutagenesis of the Mesp>*Intβ1* and Mesp>*Intβ2* expression plasmids. Mesp>*FGFR:Venus* was sub-cloned from a Brac>*FGFR:Venus* construct generously provided by Weiyang Shi. The full-length coding region of FGFR was initially amplified from EST clone GC32j14 (*Ciona intestinalis* Gene Collection Release 1; Beh et al., 2007; Satou et al., 2002) and inserted downstream of the *Brachyury* enhancer using Not1 and EcoR1. The Venus open reading frame (ORF) was then fused in frame using the EcoR1 site. *FGFR:Venus* was subsequently sub-cloned downstream of the Mesp enhancer using XbaI and Not1 sites. *Ci-Caveolin* (*CavA*) was PCR amplified from the full open reading frame unigene collection (Cogenics) clone id# VES60_PO7 and inserted into either Mesp>*GFP* or Mesp>*RFP* fusion vectors. The Mesp>*Caveolin* mutant constructs were generated by site-directed mutagenesis of the Mesp>*Caveolin* expression plasmid.

Antibody Staining and Image Analysis

Embryos were fixed and antibody stained as previously described (Cooley et al., 2011) using the following antibodies: rabbit anti-GFP (catalog no. A-11122; Life Technologies), mouse anti-GFP (catalog no. A-11120; Life Technologies), rat anti-RED (catalog no. ABIN334653; Antibodies Online), Alexa Fluor 488 anti-mouse (catalog no. A21202; Molecular Probes), Alexa Fluor 488 anti-rabbit (catalog no. A21206; Molecular Probes), Alexa Fluor 564 anti-rat (catalog no. A-21208; Molecular Probes). Alexa Fluor Phalloidin 555/633 (Molecular Probes) was used to detect F-actin. DRAQ5 (Molecular Probes) was used to detect DNA. For measurements of ventral/dorsal staining ratios, lateral optical section obtained from 1-μM confocal stacks were analyzed using ImageJ. Generation and use of the region of interest (ROI) and background subtraction tools achieved consistent outlining and detection of GFP-stained regions.

CRISPR/Cas9

U6>*sgRNA(F+E)* and Mesp>*nls::Cas9::nls* plasmids were a kind gift of Lionel Christiaen (Stolfi et al., 2014). Putative (N21)+GG exon 1 *CavA* gRNA targets were identified with Jack Lin's CRISPR/Cas9 gRNA Finder (http://spot.colorado.edu/~slin/cas9.html) and subsequently screened for off-targets and polymorphisms. gRNAs were inserted in to the empty U6>*sgRNA(F+E)* plasmid by inverse PCR. Single base mismatch mutations were introduced by site-directed mutagenesis. To assess mutagenesis of *CavA*, we amplified the presumed CRISPR target region in exon 1 using genomic DNA isolated from pooled transgenic embryos (n > 100). Targeted Caveolin genomic DNA

was amplified and cloned into pCRII-TOPO Dual-Promoter (Invitrogen) prior to sequencing.

Ex Vivo Adhesion Assays

All assays were performed as described previously (Norton et al., 2013). The raw average values ±SEM are as follows (adherent cells::estimated cell density × 10^5): Rap^{S17N} Control: 28.3.4 ± 8.7::0.63 ± 0.28; Rap^{S17N} + $Int\beta1^{Y694F}$: 51.7 ± 7.4::0.71 ± 0.26; Rap^{S17N} + $Int\beta2^{F801Y}$: 39.7 ± 13.7::0.82 ± 0.07 (Figure 3C) and Rap^{S17N} Control: 15.5 ± 1.7::2.2 ± 0.76; Rap^{S17N} + Intβ2 Control: 14 ± 0.59::1.73 ± 0.74; Rap^{S17N} + Caveolin:GFP: 20.5 ± 0.94::4.4 ± 1.9 (Figure 6E).

SUPPLEMENTAL INFORMATION

Supplemental Information includes Supplemental Experimental Procedures, six figures, and two tables and can be found with this article online at http://dx.doi.org/10.1016/j.devcel.2015.07.001.

ACKNOWLEDGMENTS

We thank Steve DiNardo, John Epstein, and Richard Behringer for their suggestions and comments on the manuscript. We also thank Emily MacDuffie for initial development of the FGFR:Venus assay and Lionel Christiaen for his generous gift of the Cas9 and sgRNA constructs. C.C. was supported by the American Heart Association Postdoctoral Award (13POST14210014). Funding was also provided by Swarthmore College and the NIH (1R01HL091027, R15 HD080525-01).

Received: August 29, 2014
Revised: April 14, 2015
Accepted: July 2, 2015
Published: August 20, 2015

REFERENCES

Anthis, N.J., Haling, J.R., Oxley, C.L., Memo, M., Wegener, K.L., Lim, C.J., Ginsberg, M.H., and Campbell, I.D. (2009). β integrin tyrosine phosphorylation is a conserved mechanism for regulating talin-induced integrin activation. J. Biol. Chem. *284*, 36700–36710.

Beh, J., Shi, W., Levine, M., Davidson, B., and Christiaen, L. (2007). FoxF is essential for FGF-induced migration of heart progenitor cells in the ascidian Ciona intestinalis. Development *134*, 3297–3305.

Boettner, B., and Van Aelst, L. (2009). Control of cell adhesion dynamics by Rap1 signaling. Curr. Opin. Cell Biol. *21*, 684–693.

Bonaventure, J., Horne, W.C., and Baron, R. (2007). The localization of FGFR3 mutations causing thanatophoric dysplasia type I differentially affects phosphorylation, processing and ubiquitylation of the receptor. FEBS J. *274*, 3078–3093.

Boucrot, E., and Kirchhausen, T. (2007). Endosomal recycling controls plasma membrane area during mitosis. Proc. Natl. Acad. Sci. USA *104*, 7939–7944.

Boucrot, E., Howes, M.T., Kirchhausen, T., and Parton, R.G. (2011). Redistribution of caveolae during mitosis. J. Cell Sci. *124*, 1965–1972.

Brunet, T., Bouclet, A., Ahmadi, P., Mitrossilis, D., Driquez, B., Brunet, A.-C., Henry, L., Serman, F., Béalle, G., Ménager, C., et al. (2013). Evolutionary conservation of early mesoderm specification by mechanotransduction in Bilateria. Nat. Commun. *4*, 2821.

Bryant, M.R., Marta, C.B., Kim, F.S., and Bansal, R. (2009). Phosphorylation and lipid raft association of fibroblast growth factor receptor-2 in oligodendrocytes. Glia *57*, 935–946.

Calderwood, D.A., Fujioka, Y., de Pereda, J.M., García-Alvarez, B., Nakamoto, T., Margolis, B., McGlade, C.J., Liddington, R.C., and Ginsberg, M.H. (2003). Integrin beta cytoplasmic domain interactions with phosphotyrosine-binding domains: a structural prototype for diversity in integrin signaling. Proc. Natl. Acad. Sci. USA *100*, 2272–2277.

Caswell, P., and Norman, J. (2008). Endocytic transport of integrins during cell migration and invasion. Trends Cell Biol. *18*, 257–263.

Caswell, P.T., Vadrevu, S., and Norman, J.C. (2009). Integrins: masters and slaves of endocytic transport. Nat. Rev. Mol. Cell Biol. *10*, 843–853.

Cerezo, A., Guadamillas, M.C., Goetz, J.G., Sánchez-Perales, S., Klein, E., Assoian, R.K., and del Pozo, M.A. (2009). The absence of caveolin-1 increases proliferation and anchorage- independent growth by a Rac-dependent, Erk-independent mechanism. Mol. Cell. Biol. *29*, 5046–5059.

Cooley, J., Whitaker, S., Sweeney, S., Fraser, S., and Davidson, B. (2011). Cytoskeletal polarity mediates localized induction of the heart progenitor lineage. Nat. Cell Biol. *13*, 952–957.

Corbo, J.C., Levine, M., and Zeller, R.W. (1997). Characterization of a notochord-specific enhancer from the Brachyury promoter region of the ascidian, Ciona intestinalis. Development *124*, 589–602.

Cota, C.D., Segade, F., and Davidson, B. (2014). Heart genetics in a small package, exploiting the condensed genome of Ciona intestinalis. Brief. Funct. Genomics *13*, 3–14.

Dave, P.C., Dingal, P., and Discher, D.E. (2014). Material control of stem cell differentiation: challenges in nano-characterization. Curr. Opin. Biotechnol. *28*, 46–50.

Davidson, B. (2007). Ciona intestinalis as a model for cardiac development. Semin. Cell Dev. Biol. *18*, 16–26.

Davidson, B., and Levine, M. (2003). Evolutionary origins of the vertebrate heart: Specification of the cardiac lineage in Ciona intestinalis. Proc. Natl. Acad. Sci. USA *100*, 11469–11473.

Davidson, B., Shi, W., and Levine, M. (2005). Uncoupling heart cell specification and migration in the simple chordate Ciona intestinalis. Development *132*, 4811–4818.

Davidson, B., Shi, W., Beh, J., Christiaen, L., and Levine, M. (2006). FGF signaling delineates the cardiac progenitor field in the simple chordate, Ciona intestinalis. Genes Dev. *20*, 2728–2738.

Dehal, P., Satou, Y., Campbell, R.K., Chapman, J., Degnan, B., De Tomaso, A., Davidson, B., Di Gregorio, A., Gelpke, M., Goodstein, D.M., et al. (2002). The draft genome of Ciona intestinalis: insights into chordate and vertebrate origins. Science *298*, 2157–2167.

del Pozo, M.A., Alderson, N.B., Kiosses, W.B., Chiang, H.-H., Anderson, R.G.W., and Schwartz, M.A. (2004). Integrins regulate Rac targeting by internalization of membrane domains. Science *303*, 839–842.

del Pozo, M.A., Balasubramanian, N., Alderson, N.B., Kiosses, W.B., Grande-García, A., Anderson, R.G.W., and Schwartz, M.A. (2005). Phospho-caveolin-1 mediates integrin-regulated membrane domain internalization. Nat. Cell Biol. *7*, 901–908.

Delcommenne, M., Tan, C., Gray, V., Rue, L., Woodgett, J., and Dedhar, S. (1998). Phosphoinositide-3-OH kinase-dependent regulation of glycogen synthase kinase 3 and protein kinase B/AKT by the integrin-linked kinase. Proc. Natl. Acad. Sci. USA *95*, 11211–11216.

Di Guglielmo, G.M., Le Roy, C., Goodfellow, A.F., and Wrana, J.L. (2003). Distinct endocytic pathways regulate TGF-beta receptor signalling and turnover. Nat. Cell Biol. *5*, 410–421.

Du, J., Chen, X., Liang, X., Zhang, G., Xu, J., He, L., Zhan, Q., Feng, X.-Q., Chien, S., and Yang, C. (2011). Integrin activation and internalization on soft ECM as a mechanism of induction of stem cell differentiation by ECM elasticity. Proc. Natl. Acad. Sci. USA *108*, 9466–9471.

Engler, A.J., Sen, S., Sweeney, H.L., and Discher, D.E. (2006). Matrix elasticity directs stem cell lineage specification. Cell *126*, 677–689.

Farge, E. (2011). Mechanotransduction in development. Curr. Top. Dev. Biol. *95*, 243–265.

Fonar, Y., Gutkovich, Y.E., Root, H., Malyarova, A., Aamar, E., Golubovskaya, V.M., Elias, S., Elkouby, Y.M., and Frank, D. (2011). Focal adhesion kinase protein regulates Wnt3a gene expression to control cell fate specification in the developing neural plate. Mol. Biol. Cell *22*, 2409–2421.

Fürthauer, M., and González-Gaitán, M. (2009). Endocytosis and mitosis: a two-way relationship. Cell Cycle *8*, 3311–3318.

Goh, L.K., and Sorkin, A. (2013). Endocytosis of receptor tyrosine kinases. Cold Spring Harb. Perspect. Biol. *5*, a017459.

Goulas, S., Conder, R., and Knoblich, J.A. (2012). The Par complex and integrins direct asymmetric cell division in adult intestinal stem cells. Cell Stem Cell *11*, 529–540.

Guadamillas, M.C., Cerezo, A., and Del Pozo, M.A. (2011). Overcoming anoikis–pathways to anchorage-independent growth in cancer. J. Cell Sci. *124*, 3189–3197.

Harvey, R.D., and Calaghan, S.C. (2012). Caveolae create local signalling domains through their distinct protein content, lipid profile and morphology. J. Mol. Cell. Cardiol. *52*, 366–375.

Hatch, N.E., Hudson, M., Seto, M.L., Cunningham, M.L., and Bothwell, M. (2006). Intracellular retention, degradation, and signaling of glycosylation-deficient FGFR2 and craniosynostosis syndrome-associated FGFR2C278F. J. Biol. Chem. *281*, 27292–27305.

Hotta, K., Mitsuhara, K., Takahashi, H., Inaba, K., Oka, K., Gojobori, T., and Ikeo, K. (2007). A web-based interactive developmental table for the ascidian Ciona intestinalis, including 3D real-image embryo reconstructions: I. From fertilized egg to hatching larva. Dev. Dyn. *236*, 1790–1805.

Hu, P., and Luo, B.H. (2013). Integrin bi-directional signaling across the plasma membrane. J. Cell. Physiol. *228*, 306–312.

Huttenlocher, A., and Horwitz, A.R. (2011). Integrins in cell migration. Cold Spring Harb. Perspect. Biol. *3*, a005074.

Ivaska, J., and Heino, J. (2011). Cooperation between integrins and growth factor receptors in signaling and endocytosis. Annu. Rev. Cell Dev. Biol. *27*, 291–320.

Kaabeche, K., Lemonnier, J., Le Mée, S., Caverzasio, J., and Marie, P.J. (2004). Cbl-mediated degradation of Lyn and Fyn induced by constitutive fibroblast growth factor receptor-2 activation supports osteoblast differentiation. J. Biol. Chem. *279*, 36259–36267.

Kim, S.-H., Turnbull, J., and Guimond, S. (2011). Extracellular matrix and cell signalling: the dynamic cooperation of integrin, proteoglycan and growth factor receptor. J. Endocrinol. *209*, 139–151.

LaFlamme, S.E., Nieves, B., Colello, D., and Reverte, C.G. (2008). Integrins as regulators of the mitotic machinery. Curr. Opin. Cell Biol. *20*, 576–582.

Lee, H., Park, D.S., Razani, B., Russell, R.G., Pestell, R.G., and Lisanti, M.P. (2002). Caveolin-1 mutations (P132L and null) and the pathogenesis of breast cancer: caveolin-1 (P132L) behaves in a dominant-negative manner and caveolin-1 (-/-) null mice show mammary epithelial cell hyperplasia. Am. J. Pathol. *161*, 1357–1369.

Legate, K.R., Wickström, S.A., and Fässler, R. (2009). Genetic and cell biological analysis of integrin outside-in signaling. Genes Dev. *23*, 397–418.

Lemaire, P. (2011). Evolutionary crossroads in developmental biology: the tunicates. Development *138*, 2143–2152.

Liu, S., Calderwood, D.A., and Ginsberg, M.H. (2000). Integrin cytoplasmic domain-binding proteins. J. Cell Sci. *113*, 3563–3571.

Martin-Bermudo, M.D. (2000). Integrins modulate the Egfr signaling pathway to regulate tendon cell differentiation in the Drosophila embryo. Development *127*, 2607–2615.

McKay, H.F., and Burgess, D.R. (2011). 'Life is a highway': membrane trafficking during cytokinesis. Traffic *12*, 247–251.

Miller, C.J., and Davidson, L.A. (2013). The interplay between cell signalling and mechanics in developmental processes. Nat. Rev. Genet. *14*, 733–744.

Monsonego-Ornan, E., Adar, R., Rom, E., and Yayon, A. (2002). FGF receptors ubiquitylation: dependence on tyrosine kinase activity and role in downregulation. FEBS Lett. *528*, 83–89.

Montagnac, G., Echard, A., and Chavrier, P. (2008). Endocytic traffic in animal cell cytokinesis. Curr. Opin. Cell Biol. *20*, 454–461.

Moser, M., Legate, K.R., Zent, R., and Fässler, R. (2009). The tail of integrins, talin, and kindlins. Science *324*, 895–899.

Nishimura, T., and Kaibuchi, K. (2007). Numb controls integrin endocytosis for directional cell migration with aPKC and PAR-3. Dev. Cell *13*, 15–28.

Norton, J., Cooley, J., Islam, A.F.M.T., Cota, C.D., and Davidson, B. (2013). Matrix adhesion polarizes heart progenitor induction in the invertebrate chordate Ciona intestinalis. Development *140*, 1301–1311.

Nowak, M., Machate, A., Yu, S.R., Gupta, M., and Brand, M. (2011). Interpretation of the FGF8 morphogen gradient is regulated by endocytic trafficking. Nat. Cell Biol. *13*, 153–158.

Parton, R.G., and del Pozo, M.A. (2013). Caveolae as plasma membrane sensors, protectors and organizers. Nat. Rev. Mol. Cell Biol. *14*, 98–112.

Patel, H.H., Murray, F., and Insel, P.A. (2008). Caveolae as organizers of pharmacologically relevant signal transduction molecules. Annu. Rev. Pharmacol. Toxicol. *48*, 359–391.

Pellinen, T., Tuomi, S., Arjonen, A., Wolf, M., Edgren, H., Meyer, H., Grosse, R., Kitzing, T., Rantala, J.K., Kallioniemi, O., et al. (2008). Integrin trafficking regulated by Rab21 is necessary for cytokinesis. Dev. Cell *15*, 371–385.

Radel, C., and Rizzo, V. (2005). Integrin mechanotransduction stimulates caveolin-1 phosphorylation and recruitment of Csk to mediate actin reorganization. Am. J. Physiol. Heart Circ. Physiol. *288*, H936–H945.

Reilly, G.C., and Engler, A.J. (2010). Intrinsic extracellular matrix properties regulate stem cell differentiation. J. Biomech. *43*, 55–62.

Salanueva, I.J., Cerezo, A., Guadamillas, M.C., and del Pozo, M.A. (2007). Integrin regulation of caveolin function. J. Cell. Mol. Med. *11*, 969–980.

Sasaki, H., Yoshida, K., Hozumi, A., and Sasakura, Y. (2014). CRISPR/Cas9-mediated gene knockout in the ascidian Ciona intestinalis. Dev. Growth Differ. *56*, 499–510.

Satou, Y., Yamada, L., Mochizuki, Y., Takatori, N., Kawashima, T., Sasaki, A., Hamaguchi, M., Awazu, S., Yagi, K., Sasakura, Y., et al. (2002). A cDNA resource from the basal chordate Ciona intestinalis. Genesis *33*, 153–154.

Schmidt-Glenewinkel, H., Reinz, E., Bulashevska, S., Beaudouin, J., Legewie, S., Alonso, A., and Eils, R. (2012). Multiparametric image analysis reveals role of Caveolin1 in endosomal progression rather than internalization of EGFR. FEBS Lett. *586*, 1179–1189.

Shatz, M., Lustig, G., Reich, R., and Liscovitch, M. (2010). Caveolin-1 mutants P132L and Y14F are dominant negative regulators of invasion, migration and aggregation in H1299 lung cancer cells. Exp. Cell Res. *316*, 1748–1762.

Shibue, T., and Weinberg, R.A. (2009). Integrin beta1-focal adhesion kinase signaling directs the proliferation of metastatic cancer cells disseminated in the lungs. Proc. Natl. Acad. Sci. USA *106*, 10290–10295.

Shrestha, R., Little, K.A., Tamayo, J.V., Li, W., Perlman, D.H., and Devenport, D. (2015). Mitotic control of planar cell polarity by Polo-like Kinase 1. Dev. Cell *33*, 522–534.

Singh, R.D., Holicky, E.L., Cheng, Z.-J., Kim, S.-Y., Wheatley, C.L., Marks, D.L., Bittman, R., and Pagano, R.E. (2007). Inhibition of caveolar uptake, SV40 infection, and beta1-integrin signaling by a nonnatural glycosphingolipid stereoisomer. J. Cell Biol. *176*, 895–901.

Stolfi, A., and Christiaen, L. (2012). Genetic and genomic toolbox of the chordate Ciona intestinalis. Genetics *192*, 55–66.

Stolfi, A., Gandhi, S., Salek, F., and Christiaen, L. (2014). Tissue-specific genome editing in Ciona embryos by CRISPR/Cas9. Development *141*, 4115–4120.

Strålfors, P. (2012). Caveolins and caveolae, roles in insulin signalling and diabetes. Adv. Exp. Med. Biol. *729*, 111–126.

Streuli, C.H. (2009). Integrins and cell-fate determination. J. Cell Sci. *122*, 171–177.

Streuli, C.H., and Akhtar, N. (2009). Signal co-operation between integrins and other receptor systems. Biochem. J. *418*, 491–506.

Tacheva-Grigorova, S.K., Santos, A.J.M., Boucrot, E., and Kirchhausen, T. (2013). Clathrin-mediated endocytosis persists during unperturbed mitosis. Cell Rep. *4*, 659–668.

Teckchandani, A., Toida, N., Goodchild, J., Henderson, C., Watts, J., Wollscheid, B., and Cooper, J.A. (2009). Quantitative proteomics identifies a Dab2/integrin module regulating cell migration. J. Cell Biol. *186*, 99–111.

Toyoshima, F., and Nishida, E. (2007). Spindle orientation in animal cell mitosis: roles of integrin in the control of spindle axis. J. Cell. Physiol. *213*, 407–411.

Wickström, S.A., Lange, A., Hess, M.W., Polleux, J., Spatz, J.P., Krüger, M., Pfaller, K., Lambacher, A., Bloch, W., Mann, M., et al. (2010). Integrin-linked kinase controls microtubule dynamics required for plasma membrane targeting of caveolae. Dev. Cell *19*, 574–588.

Woznica, A., Haeussler, M., Starobinska, E., Jemmett, J., Li, Y., Mount, D., and Davidson, B. (2012). Initial deployment of the cardiogenic gene regulatory network in the basal chordate, Ciona intestinalis. Dev. Biol. *368*, 127–139.

Yamashita, Y.M., Yuan, H., Cheng, J., and Hunt, A.J. (2010). Polarity in stem cell division: asymmetric stem cell division in tissue homeostasis. Cold Spring Harb. Perspect. Biol. *2*, a001313–a001313.

Yim, E.K.F., and Sheetz, M.P. (2012). Force-dependent cell signaling in stem cell differentiation. Stem Cell Res. Ther. *3*, 41.

Zhou, Y., Liang, H., Rodkey, T., Ariotti, N., Parton, R.G., and Hancock, J.F. (2014). Signal integration by lipid-mediated spatial cross talk between Ras nanoclusters. Mol. Cell. Biol. *34*, 862–876.